

# Old reserves and ancient buds fuel regrowth of coast redwood after catastrophic fire

Received: 31 May 2023

Accepted: 1 November 2023

Published online: 30 November 2023

 Check for updates

Drew M. P. Peltier<sup>1</sup>✉, Mariah S. Carbone<sup>1</sup>, Melissa Enright<sup>2</sup>, Margaret C. Marshall<sup>3</sup>, Amy M. Trowbridge<sup>3</sup>, Jim LeMoine<sup>1</sup>, George Koch<sup>1</sup> & Andrew D. Richardson<sup>1</sup>

For long-lived organisms, investment in insurance strategies such as reserve energy storage can enable resilience to resource deficits, stress or catastrophic disturbance. Recent fire in California damaged coast redwood (*Sequoia sempervirens*) groves, consuming all foliage on some of the tallest and oldest trees on Earth. Burned trees recovered through resprouting from roots, trunk and branches, necessarily supported by nonstructural carbon reserves. Nonstructural carbon reserves can be many years old, but direct use of old carbon has rarely been documented and never in such large, old trees. We found some sprouts contained the oldest carbon ever observed to be remobilized for growth. For certain trees, simulations estimate up to half of sprout carbon was acquired in photosynthesis more than 57 years prior, and direct observations in sapwood show trees can access reserves at least as old. Sprouts also emerged from ancient buds—dormant under bark for centuries. For organisms with millennial lifespans, traits enabling survival of infrequent but catastrophic events may represent an important energy sink. Remobilization of decades-old photosynthate after disturbance demonstrates substantial amounts of nonstructural carbon within ancient trees cycles on slow, multidecadal timescales.

Nonstructural carbon (mainly sugars and starch) is often considered a rapidly cycling pool of transient reserves in woody plants<sup>1–3</sup>. Consistent with this generalization, carbon in leaves, actively growing tissues and respired CO<sub>2</sub> is often ‘young’, a product of recent photosynthesis<sup>4</sup>. However, reserves in other tissues accumulate through many years and can be old, particularly in long-lived plants such as trees<sup>5</sup>. The conditions under which these old reserves accumulate and are depleted are unclear. One interpretation of the accumulation of carbon reserves is that carbon is rarely a limiting resource on annual timescales, and reserves represent an excess of carbon supply versus demand<sup>6</sup>. Over tree lifespans, however, such reserves may be essential to respond to infrequent, high-severity disturbances that reduce photosynthetic capacity. Pest outbreaks, fire and hurricanes destroy foliage and often cause sustained reductions in tree growth<sup>7–9</sup>. Stored carbon reserves may then serve as emergency energy supply following catastrophic

disruption of tree carbon balance<sup>10</sup>. Newly grown fine roots following hurricanes<sup>11</sup> or stump sprouts following tree harvesting<sup>5</sup> can be made of carbon fixed from the atmosphere many years prior. Previous work has been limited to relatively young trees (hundreds of years old), yet some tree species can live for thousands of years, raising the possibility of exceptionally old carbon reserves serving as a mechanism enabling resilience to disturbance across extreme lifespans.

Coast redwood (*Sequoia sempervirens* (D. Don) Endl.) can live over 2,500 years, is the tallest and second largest tree species on Earth<sup>12</sup> and is one of few charismatic mega-flora. Like their stature, the carbon economy of redwood trees is similarly superlative—a single large individual (91 m tall, -7 m diameter, -1,200 years old) was estimated to have an annual aboveground biomass increment as high as 0.77 Mg per year<sup>13</sup>, similar to the annual net ecosystem production of 1 ha of certain eastern temperate forests<sup>14</sup>. Redwood also exhibits a suite of

<sup>1</sup>Center for Ecosystem Science and Society, Northern Arizona University, Flagstaff, AZ, USA. <sup>2</sup>Pacific Northwest Research Station, US Forest Service, Portland, OR, USA. <sup>3</sup>Department of Forest and Wildlife Ecology, University of Wisconsin-Madison, Madison, WI, USA. ✉e-mail: [dmp334@nau.edu](mailto:dmp334@nau.edu)

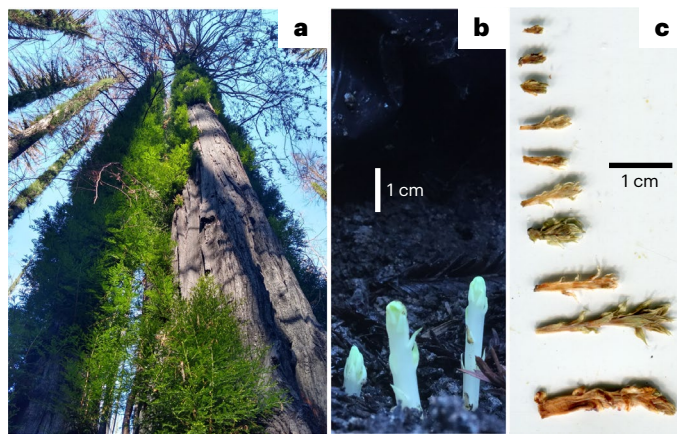


**Fig. 1** | The CZU Lightning Complex fire burned through BBRSP on 18 August 2020. **a–c**, Fire burned into tree canopies and destroyed all foliage in most trees (Supplementary Fig. 1). **a**, Surviving trees produced epicormic sprouts prolifically post-fire (image: April 2022), from roots, bole and branches. **b,c**, We analysed the  $\Delta^{14}\text{C}$  of sprouts grown in the dark under opaque plastic (**b**), which were frequently very small (**c**).

traits enabling resilience to fire such as extremely thick bark and, critically, the capacity to resprout from roots, main stem and branches<sup>15</sup>. Although redwood occurs naturally in generally mesic environments, a history of low-severity fire is well documented throughout the species' range with fire return intervals of 8–20 years, particularly before widespread fire suppression<sup>16,17</sup>. A 1,000-year-old tree may then have experienced as many as 100 fires, with some potentially triggering resprouting behaviour<sup>15,18</sup>. While individual resilience to low-intensity wildfire may determine how rapidly a tree regains pre-disturbance function (for example, growth rate), resilience to high-intensity, crown-destroying wildfire is simply surviving the event. Is the resilience to such extreme fire in redwoods enabled by the mobilization of exceptionally old carbon reserves? A catastrophic high-severity fire at Big Basin Redwoods State Park (BBRSP), California, in August 2020 provided an opportunity to answer this question.

While wildfire is a common occurrence in California<sup>16</sup>, fires of the size and severity that swept through the redwood groves in the summer of 2020 are rare. Of the ten largest wildfires in California history, five occurred in 2020, and some of the impacts of this extreme fire year were unprecedented since Euro-American settlement<sup>19</sup>. In August 2020 the 'CZU Lightning Complex' fire burned through remnant old-growth redwood forest in BBRSP, and many trees' crowns were burned, including some >90-m-tall trees, resulting in total loss of canopy leaves. Similar to most coast redwood groves, this area had not burned at such high intensity for at least a century<sup>20</sup>. In the stands we studied, all co-occurring Douglas fir (*Pseudotsuga menziesii*), which cannot resprout, died in the fire, including large individuals that were at least 150 years old.

Despite the immense damage to the forest and to park infrastructure (Supplementary Fig. 1), this event presented a unique opportunity to study the use of carbon reserves for post-fire recovery in some of the tallest and oldest trees on Earth. Many redwoods survived the fire to subsequently produce new shoots and leaf tissue via prolific epicormic resprouting, by necessity supported by reserves because photosynthesis was halted due to complete canopy loss (Fig. 1). We sought to understand the physiology of this unique disturbance and recovery event by characterizing the age of carbon reserves remobilized for resprouting. Four months after the fire, we covered small basal buds on burnt trees to exclude light (arresting photosynthesis) and ensure sprouts were grown entirely using stored carbon reserves. We collected sprouts over the following 6 months (Fig. 1b,c). We used radiocarbon ( $\Delta^{14}\text{C}$ )

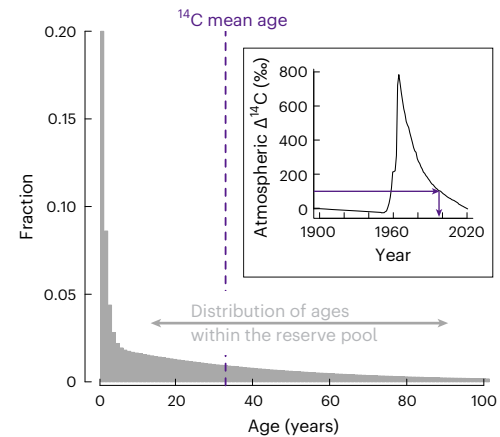


**Fig. 2** | Radiocarbon ( $^{14}\text{C}$ ) levels in the atmosphere spiked in the early 1960s following atmospheric thermonuclear bomb testing, and incorporation of this bomb carbon into tree carbon reserves provides information on the age of reserves. Because trees continuously add new photosynthate to carbon reserve pools, the distribution of reserves is primarily young. Radiocarbon dating of reserve carbon (or a sprout) can only provide information on the  $^{14}\text{C}$  mean age of this pool. Modelling or simulations are required to understand the distribution of ages within reserve pools.

to determine the mean age (or time since photosynthetic fixation) of sprout carbon by reference to the atmospheric bomb spike (Fig. 2)<sup>21,22</sup>.

## Results and discussion

### Old carbon reserves fuel resprouting

Six months after the fire, some sprouts were built from the oldest carbon ever observed to be remobilized for plant growth, with a  $^{14}\text{C}$  mean age upwards of 20 years old (Fig. 3). In past work, reserve carbon stored in temperate trees' stem wood had a  $^{14}\text{C}$  mean age of 7–14 years<sup>23</sup>, while sugars remobilized for spring leaf flushing<sup>24</sup> or refoliation following late frost<sup>25</sup> had a  $^{14}\text{C}$  mean age of 3–5 years. Trees have remobilized older reserves following more extreme events, where stump sprouts from harvested trees had a maximum  $^{14}\text{C}$  mean age of 17 years<sup>5</sup>, and respired carbon from dying, girdled trees had  $^{14}\text{C}$  mean ages as high as 13–14 years<sup>26</sup>. Here, in the oldest and largest trees in which carbon reserve ages have been assessed, the sprout comprising the oldest carbon we collected had a  $^{14}\text{C}$  signature that dates to the year 2000 on the bomb spike, or a  $^{14}\text{C}$  mean age of  $21 \pm 0.5$  years ( $\Delta^{14}\text{C} = 85 \pm 2\text{‰}$ ; Fig. 3). Given the trees' large size (Fig. 1), there was variability in  $^{14}\text{C}$  mean age of sprouts collected from a given individual, where replicate measurements within a sprout varied by 2.8‰ (up to 4.8‰) but varied across sprouts collected from the same tree by 5.1‰ (up to 21.3‰). While some sprouts comprised old carbon, many comprised very young carbon, in which the average of all sprout  $^{14}\text{C}$  mean ages was 7.5 years ( $\Delta^{14}\text{C} = 24 \pm 19\text{‰}$ ;  $n = 99$ ). For example, some sprouts had  $\Delta^{14}\text{C}$  as low as  $-3\text{‰}$ , apparently reflecting the 2020 atmosphere, or only 1-year-old carbon.

Living parenchyma cells of sapwood, the water-conducting vascular tissue surrounding metabolically inactive heartwood, represent one major pool of carbon reserves that may support resprouting. We found evidence that larger trees with deeper sapwood contained older reserves ( $P < 0.001$ , linear regression,  $R^2 = 0.59$ ; Supplementary Fig. 2) and produced older sprout  $^{14}\text{C}$  mean ages. Sprout  $^{14}\text{C}$  mean age was older in trees with more sapwood tree rings, particularly if the sole sampled tree with fire-damaged xylem was excluded ( $P < 0.01$ ,  $R^2 = 0.35$ ; Supplementary Fig. 2). This is likely because sprout  $^{14}\text{C}$  mean age was significantly related to both the age and size of the sapwood carbon reserve pool, where trees with smaller reserve pools ( $R^2 = 0.35$ ) and older reserve pools ( $R^2 = 0.39$ ) tended to produce older sprout  $^{14}\text{C}$

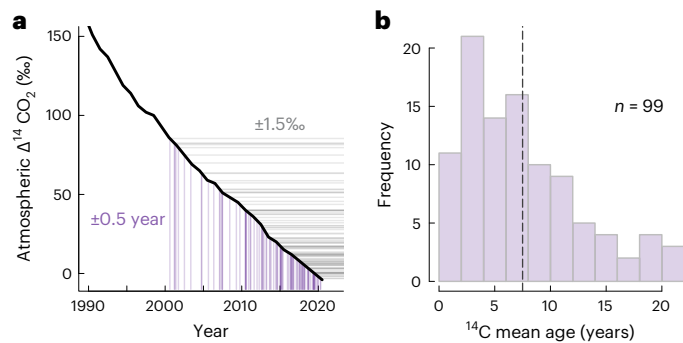


**Fig. 3 | Post-fire sprouts were built from reserve carbon with a  $^{14}\text{C}$  mean age (reserve carbon is a heterogeneous mixture) from 1 to 21 years old. a**, By matching  $\Delta^{14}\text{C}$  of sprouts (grey horizontal lines) to the atmospheric bomb spike (thick black line; Hua et al.<sup>22</sup>) we estimated the mean date of photosynthetic fixation from the atmosphere for each sprout (vertical purple lines). **b**, This  $^{14}\text{C}$  mean age was as high as  $21 \pm 0.5$  years, with an average across all measured sprouts of  $7 \pm 5$  years (vertical dashed line). We report uncertainty for individual observations as analytical (accelerator mass spectrometry, AMS) uncertainty in Supplementary Table 1 (averaging 1.5‰ or 0.5 years). Reserve carbon is a heterogeneous mixture because before fire, young carbon was constantly being added to the pool each year over many years (Fig. 2). A radiocarbon measurement only captures the mean age of this mixture (reported here), where some carbon in the mixture may be very young/old. Notes: In a atmospheric  $\Delta^{14}\text{C}$  record was extended by 1 year to 2020 by assuming the atmosphere was  $-4\%$ , consistent with annual declines of approximately  $-4\%$  for the preceding 5–6 years. In **b** where multiple sprouts or subsamples were run from a given tree and collection date, these were aggregated into a single average value here. Full radiocarbon data reported in Supplementary Information.

mean ages ( $P < 0.01$ ; Supplementary Fig. 2). In short, sapwood carbon reserves are one probable source of carbon used to build sprouts, while other tree size or vigor metrics were not significantly related to or even moderately predictive of  $^{14}\text{C}$  mean ages (Supplementary Fig. 3). The oldest reserves occur in the deepest sapwood<sup>23</sup>, so the maximum age of tree carbon reserves may be constrained by the age of the oldest sapwood ring. Large redwood trees can have many sapwood rings (100+ here), suggesting less constraint on maximum reserve age in these large and ancient trees compared to previous studies (for example, less than 10 rings in *Pinus strobus* and *Quercus rubra*<sup>23</sup>). In this context, simulations may be useful to quantify the age of potential sources of sapwood carbon reserves for sprout growth.

### Carbon reserve pools are heterogeneous mixtures

Radiocarbon dating relies on the overall ratio of  $^{14}\text{C}$  to  $^{12}\text{C}$  in a sample, and it offers a measure of the mean age of a sample, whether that mean age is estimated from the bomb spike or from calibrated, pre-bomb chronologies (Fig. 2)<sup>21</sup>. While this estimate is highly certain in the sense of instrument precision and accuracy, radiocarbon dating is unable to provide information about the age of individual carbon atoms within a mixture or the distribution of ages within a sample. Tree carbon reserves are built up over many years and thus comprise a mixture of carbon of different ages, including some which may be very old—modeling can be used to put reasonable constraints on the distribution of these ages<sup>27,28</sup>. We used a simple, two-pool model of stem nonstructural carbon: (1) a ‘fast’ turnover pool of young (recently fixed) carbon and (2) a ‘slow’ turnover pool of old carbon (Fig. 4a)<sup>23</sup>. By analogy to personal finance, these may be envisioned as ‘checking’ and ‘savings’ accounts, respectively. We simulated a range of possible distributions of slow pool ages that, when mixed with different amounts of young carbon, could realistically produce  $^{14}\text{C}$  mean ages of 5, 10, 15, or 21 years as observed in sprouts (Fig. 4b).

All models producing a  $^{14}\text{C}$  mean age matching the oldest sprout ( $\Delta^{14}\text{C} = 85 \pm 2\%$ ; 21 years) implied 31–79% of remobilized carbon was

more than 20 years old, while 4–52% of that carbon was older than 57 years (Fig. 4c). These proportions did not meaningfully change ( $\pm 4\%$ ) with fast pool (‘checking account’) turnover times as long as 5 years. Fifty-seven years before our collection year of 2021 corresponds closely to the peak of the bomb spike in 1963<sup>22</sup>, before which (pre-1955) the atmosphere had  $\Delta^{14}\text{C}$  similar to recent years. Simulated incorporation of some of this ‘pre-bomb’ carbon ( $\Delta^{14}\text{C} = -0\%$ ) dilutes (reduces) total reserve  $\Delta^{14}\text{C}$ , producing the curving in Fig. 4b. Given continual annual addition of new photosynthate to carbon reserves, reserves are unlikely to be composed entirely of old carbon (that is, slow pool proportion close to 1; Fig. 4b). For a reserve pool with mean age of 21 years ( $\Delta^{14}\text{C} = 85\%$ ), intermediate mixtures contain substantial amounts of carbon older than 57 years. The oldest sprouts were then likely built with some photosynthate stored before the bomb spike occurred, fixed from the atmosphere perhaps 57–100 years ago (Fig. 4c). We note the mixture of carbon reserve ages is much more difficult to constrain for lower  $\Delta^{14}\text{C}$  values (for example,  $\Delta^{14}\text{C} = 12.5\%$ , Fig. 4b; or  $\Delta^{14}\text{C} = -3\%$ , Fig. 3b), so we assume these samples most likely comprise primarily younger carbon.

### Old reserves in tree sapwood

As additional evidence that sprouts can access very old carbon reserves, we also collected increment cores of sapwood directly adjacent to sprout collection sites on a subset of trees. We then measured the  $\Delta^{14}\text{C}$  of carbon in  $\text{CO}_2$  respired from the living cells within these sapwood cores using live-tissue incubations<sup>29</sup>. The  $^{14}\text{C}$  mean age of carbon respired from deep sapwood tree rings commonly exceeded that of the sprouts we measured, supporting our modeling approach that assumed sprouts relied on a mix of old and young carbon reserves. Carbon respired from a subsample of sapwood (rings 48–57; counted) in one 80-m-tall tree had  $\Delta^{14}\text{C} = 157 \pm 3\%$  with a  $^{14}\text{C}$  mean age of 32 years (Supplementary Fig. 4). Deeper sapwood rings in this same tree contained reserve carbon with declining  $\Delta^{14}\text{C}$ , indicating increasing incorporation of pre-bomb carbon more than 57 years old, a pattern seen across multiple trees and replicates. Thus, both direct observations and simulations suggest some trees contain labile reserve carbon photosynthesized from the atmosphere more than 57 years ago. Sprouts then may draw on a mix of reserves (Fig. 4a) including very recently fixed carbon as well as very old photosynthate.

### Sprouts arise from ancient buds

Beyond the use of such old carbon reserves for new tissue growth, the resprouting we observed stretches our understanding of the limits to resilience in a second way. Many of the epicormic sprouts observed in our study appear to be derived from ancient meristematic tissue (Fig. 5). Cross sections of fallen tree trunks we collected were traversed by axillary bud traces beneath all sprouts we examined. These traces record the annual position of buried buds moving laterally to maintain a position outside of the xylem but directly beneath the phloem<sup>30</sup>. Based on a count of annual growth rings, one sprout we observed (Fig. 5b,c) originated from a meristem that is around 600 years old. We also observed and collected sprouts emerging from the main stem of trees with ages likely exceeding 1,000 years (Fig. 5d; basal diameter ~4.5 m)—likely emerging from buried buds traversing hundreds of rings of sapwood growth during the last millennium. While dormant buds are well known, typically in younger trees<sup>30</sup>, the presence of these features in trees of such great ages may be considered an extreme example of bud longevity. Resprouting capacity, particularly from the main bole, is characteristic of trees growing in fire-prone environments, for example, many *Eucalyptus* spp. including *Eucalyptus regnans* (though it may be less important in this species)<sup>31</sup> and some *Quercus* spp. such as *Quercus suber*, but is uncommon in *Pinus* spp.<sup>32</sup>. Bole resprouting can also occur after lightning in some tropical trees<sup>33</sup>, while the capacity to resprout from basal or underground tissues is more common and widespread in angiosperms and shrubs, for example, in fire-prone systems

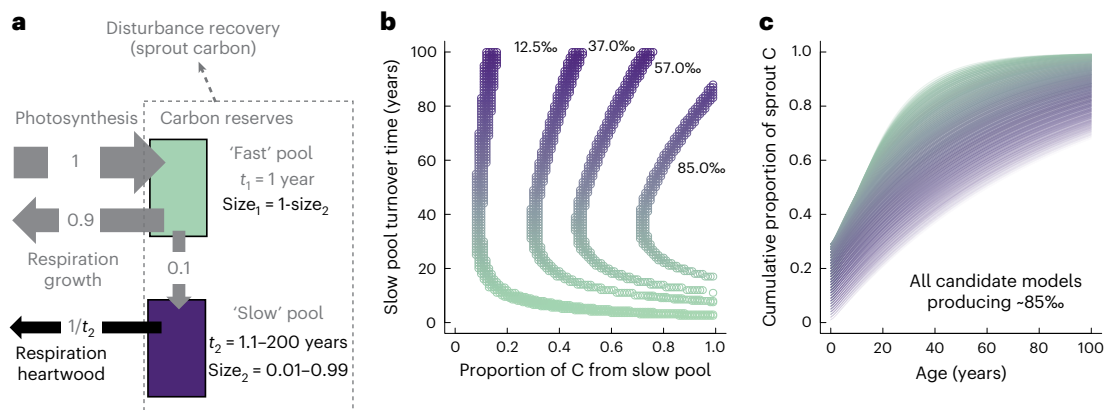


**Fig. 4 | Some trees built new tissues with carbon reserves fixed before the peak of the bomb spike (1963); these reserves are at least 57 years old.**

**a**, We simulated 10,791 candidate two-pool models, varying both size of the old pool (as the proportion of total reserves; 0.01–0.99) and turnover time of the old pool ( $t_2$ ; 1.1–100 years, younger/faster turnover shown as greens, older/slower turnover as purples) in the 'SoilR' package in R<sup>48</sup>. **b**, We then identified mixtures yielding total reserve pool ages of 5 years (12.5%), 10 years (37.0%), 15 years (57.0%) and 21 years (85.0%) (matching the highest  $\Delta^{14}\text{C}$  we observed for a sprout  $\Delta^{14}\text{C} = 85 \pm 2\%$ ; that is, between 83% and 87%); note this line curves as

more pre-bomb carbon is incorporated (longer slow pool turnover time). **c**, For the oldest sprout ( $85 \pm 2\%$ ), the cumulative sum of the density distribution (that is, the proportion of C of a given age) of the slow pool shows that 57-year-old reserves ('pre-bomb') are present in reserve pools in substantial amounts (roughly 5–50%) regardless of model formulation. In **c** line transparency is related to how much of total reserves are accounted for by the slow pool, because we assume formulations where slow pool C is nearly 100% of reserve carbon to be least biologically realistic (line shown as more transparent) compared to those with more balanced proportions of each pool (line shown as more opaque).

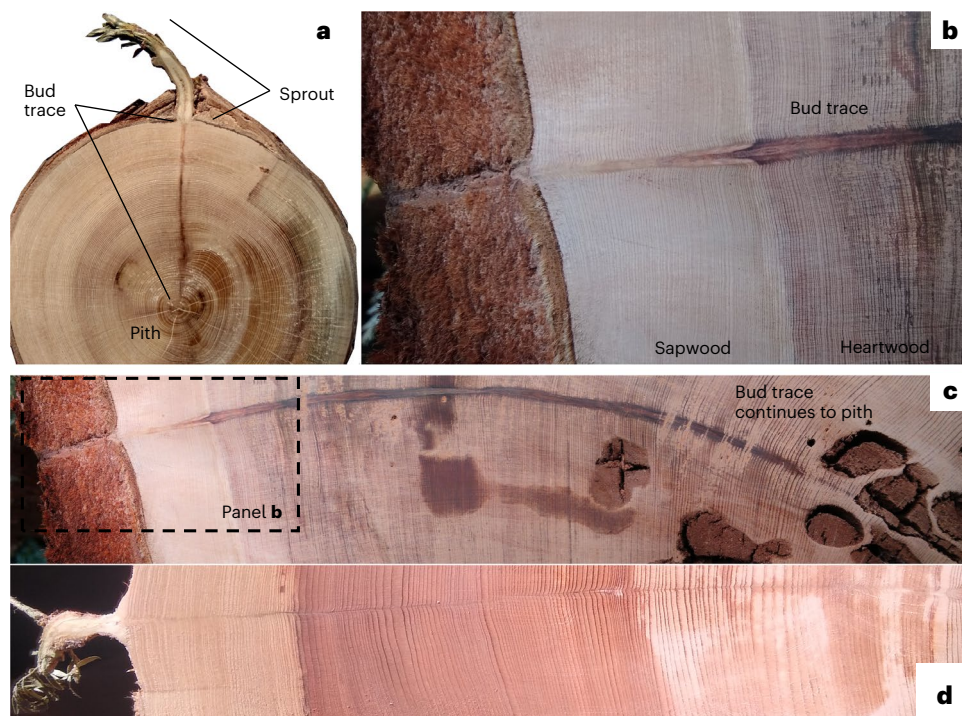


**Fig. 5 | Sprouts arose from ancient buds. a–d**, Visible here are bud traces (also known as vascular traces), showing the history of annual positions of axillary or 'buried' buds on a branch with more than 150 rings (**a**), the main stem of a fallen tree with more than 600 rings (**b**, **c**), and a partial section (0.33 m) containing more than 250 rings from a second, larger fallen tree (4.5 m basal diameter) (**d**). The section shown in **b** (sapwood) and **c** (entire cross section) was 0.91 m

in diameter at an unknown height (the tree had fallen across a park road). The section shown in **d** was collected roughly 10 m along the second fallen tree from the base. We examined branches (using cross-sections) and main stems (partial sections or 12 mm increment cores) for evidence of bud traces, in which they were universally present beneath sprouts we examined. Some trees in BBRSP exceed 1,500 years of age.

such as chaparral or savanna<sup>34</sup>. In *S. sempervirens*, the coupling of such anatomical (very long-term maintenance of emergency bud tissue) and physiological (very old carbon reserves) traits is likely a critical component of coast redwood's exceptional ability to recover from fire, while protecting long-term investments in extreme tree height.

Evidence of very old nonstructural carbon reserves and the longevity of buried buds extend current understanding of the resilience of long-lived trees. Old-growth *S. sempervirens* hold massive pools of reserve carbon, some of which is even older than sprout carbon (Supplementary Fig. 4). Using concentration measurements of

sapwood nonstructural carbohydrates (mean = 1.75–4.5% (ref. 35) depending upon assay; Supplementary Fig. 4) and published sapwood density estimates ( $350 \text{ kg m}^{-3}$  for this latitude)<sup>36</sup>, along with the published mean sapwood volume from 114 coast redwoods (including some in the same stand at BBRSP;  $33.9 \text{ m}^3$ )<sup>37</sup>, we estimate an average tree may contain 210–530 kg of reserve carbon in sapwood. If the oldest sprouts we measured are not uncommon, a single tree might hold 100–250 kg of 50+ year-old reserve carbon. Extensive storage of very old reserves is consistent with massive post-fire resprouting being a key factor driving population dynamics in coast redwood, where vegetative clones are widespread<sup>38</sup>. Even the low end of total reserves above (210 kg) is 2 million times the dry mass of a 5 cm sprout (~100 mg), providing enormous capacity for tissue regeneration such as we observed (Fig. 1a). While most photosynthetic carbon is either allocated to growth or rapidly respired back to the atmosphere, *S. sempervirens* stores photosynthate for many decades as a mechanism for resilience to fire and other disturbances. It remains unknown what roles, if any, such old reserves play in routine metabolism either seasonally or during periods of carbon deficit such as drought. Following the same calculations above, hundreds of kilograms of 1-year-old carbon reserves are present to support routine metabolism. However, a 'savings account' of hundreds of kilograms of decades-old carbon remains accessible to fuel regrowth from ancient meristematic tissue for recovery from catastrophic disturbance. Coast redwood is a large and long-lived species with large pools of carbon reserves, but other tree species are similarly long-lived or sized (for example, *Pinus longaeva*, *Pinus heldreichii*, *Fitzroya cupressoides*, *E. regnans*, *Sequoiadendron giganteum*, *Juniperus grandis*, *Taxodium distichum*) and thus may also contain very old reserves; however, this has yet to be assessed. Insurance towards long-term resilience may thus represent an important sink of tree reserve carbon over long timescales in diverse tree species, a critical and understudied component of tree resilience and longevity.

## Methods

### CZU Lightning Complex Fire and collection of sprouts

BBRSP (37.1723°N, -122.2219°W) is the oldest state park in California, USA, established in 1902 to protect old-growth redwood groves, which cover 4,400 ha. The park features the largest continuous stands of ancient (1,000–2,500 years old) redwoods south of San Francisco, and the tallest tree at BBRSP ('Mother of the Forest') previously exceeded 100 m before storm damage (now ~90 m); three of the trees we sampled exceed 80 m in height. The mean annual precipitation at the park is 490 mm, and the mean daily temperature is 20.2 °C in July and -0.3 °C in January (1991–2020 normals<sup>39</sup>). Substantial additional moisture inputs occur through frequent fog events<sup>40</sup>.

On 19 August 2020, the CZU Lightning Complex Fire burned through the forest at BBRSP, and old-growth stands at BBRSP were subjected to fires of varying intensity; the crowns of many trees were fully consumed. We visited the site on six dates during the winter, spring and early summer of 2021. We identified 60 potential study trees that already had some evidence of resprouting and measured the diameter at 1.3 m height; most trees had large buttresses. In December, any existing sprouts were cut back, and then portions of tree main stems were covered with  $\sim 1 \text{ m}^2$  dark plastic topped with reflectix (Reflectix) to exclude light and limit heating. These were revisited in February, March, April and July (roughly monthly) when sprouts were collected and subsequently oven dried at 60 °C. Some trees had multiple rounds of sprouts collected, and sprouts were collected from both the main stem and root collar. We subsequently focused our analyses on sprouts collected in February and July 2021 (first and last collection dates). To assess within-sprout and among-sprout (that is, within-tree) uncertainty in sprout ages, we also analysed tissue from some sprouts multiple times (that is, re-runs; two to three replicates each for 12 sprouts) or analysed multiple sprouts from some trees (that is, new runs; 29 samples across 14 trees, mostly three sprouts per tree).

We then calculated standard deviations of measured  $\Delta^{14}\text{C}$  across replicates within sprouts or within trees and report these as within-sprout and within-tree uncertainty. There were obvious differences in the number of sprouts produced by different trees, which we attempted to quantify in April 2021 using a categorical index of vigor from one (few sprouts) to five (many sprouts) for both the base of the tree and the main stem. Fire recovery is ongoing in this grove (Supplementary Fig. 1), and we assume that carbon dynamics at the base of the stem are reflective of resprouting dynamics occurring across the whole tree, as it was too dangerous to climb most of these fire-damaged trees.

### Direct observation of sapwood reserves

In April 2021, we identified a subset of 18 study trees to sample for main stem respired  $\text{CO}_2$  for radiocarbon and also revisited these trees in April 2022. Thus, directly adjacent to the site of sprout sampling, we collected 12 mm increment cores using an unlubricated (pure ethanol-washed) increment borer (Mattson) from each tree. Immediately after core collection, the heartwood was separated with an unlubricated razor blade and discarded, and the living tissue from these cores was similarly sliced into three sections. First was the whole bark including living phloem and periderm (hereafter 'phloem'). The sapwood was then subdivided into either halves (April 2021) or eighths (April 2022). Subsamples were subsequently incubated in 256 ml mason jars (half pint) as soon as possible after core collection (in all cases less than 30 min) to sample  $\text{CO}_2$  produced from cellular respiration of reserve carbon stored in these tissues<sup>29</sup>. Previous work showed such incubations consume reserve carbon (for example, sugars, starch) with negligible contribution of microbial decomposition<sup>29</sup>. These jars are subsequently sealed with custom two-port lids, and atmospheric  $\text{CO}_2$  in the headspace was removed by pumping air through a scrubbing column with a 'Flux Puppy' system equipped with an infra-red gas analyser<sup>41</sup>. After 120 h (5 days) headspace air containing respired  $\text{CO}_2$  was collected into 1 l gas stabilizer cans (X21L-1002, LabCommerce; ~4 times the volume of incubation jars) and subsequently  $\text{CO}_2$  was purified on a vacuum line.

We similarly collected replicate 5.15 mm increment cores, which were flash frozen after collection and subsequently freeze dried then sub-sectioned to match sectioning of the 12 mm cores above. These samples were ground on a Retsch ball mill (Retsch MM200 Ball Mill) to a fine powder. Samples were subsequently analysed following the standard phenol-sulfuric acid method<sup>42</sup>. In this method, sugar concentrations are measured following ethanol extractions (three rounds at 80 °C) via colour formation with phenol and concentrated sulfuric acid by reference to a standard curve using a spectrophotometer (GENESYS 10S UV-Vis, Thermo-Fisher Scientific). Starch concentrations are measured similarly following enzymatic digestion of the pellet remaining after sugar extraction with a mix of  $\alpha$ -amylase and amyloglucosidase (Thermo-Fisher Scientific).

We also repeated these concentration measurements using the standard enzymatic method<sup>42</sup>. This method quantifies only simple sugars (glucose, fructose and sucrose) and starch. Following three rounds of ethanol extractions at 90 °C, NAD-linked enzymatic assays are employed to convert sugars to gluconate-6-P. This reaction is directly proportional to the simultaneous reduction of NAD<sup>+</sup> to NADPH, resulting in an increase in absorbance measured at 340 nm using a spectrophotometer (Epoch, BioTek Instruments). Starch concentrations are measured through the above reactions following digestion of the pellet remaining after sugar extraction with  $\alpha$ -amylase and then amyloglucosidase (Thermo-Fischer Scientific). Sugars (glucose, fructose and sucrose) and starch are all quantified using a standard curve derived from a glucose standard solution.

### Accelerator mass spectrometry and $^{14}\text{C}$ dating

Sprouts were inspected under a dissecting microscope and, when necessary, brushed of ash and rinsed with distilled water, after which

subsamples of ~4 mg were excised with an ethanol-wiped stainless steel blade, weighed on a microbalance and rolled into tin capsules. Tin capsules were serially combusted to CO<sub>2</sub>, and CO<sub>2</sub> was graphitized on an IonPlus AGE-3 (Automated Graphitization Equipment) system. Purified CO<sub>2</sub> from incubations of 12 mm tree cores was manually graphitized in the presence of iron catalyst and hydrogen at high temperature following standard methods<sup>43,44</sup>. Graphite from sprouts and incubations was analysed for <sup>14</sup>C content on a MICADAS (Mini Carbon Dating System) (IonPlus; Synal et al.<sup>45</sup>) at the Arizona Climate and Ecosystems isotope laboratory at Northern Arizona University (Flagstaff, AZ, USA). Values are corrected for mass-dependent fractionation by normalizing to common δ<sup>13</sup>C (−25‰) under the assumption that <sup>14</sup>C fractionates twice as much as <sup>13</sup>C (ref. 46). Data are reported as decay-corrected Δ<sup>14</sup>C (‰) according to ref. 47, and Fraction Modern (F<sup>14</sup>C) values—as the sample ratio of <sup>14</sup>C/<sup>12</sup>C divided by that of a standard—are reported in Supplementary Table 1. We estimate <sup>14</sup>C mean ages (years since fixation) from Δ<sup>14</sup>C by comparing to an annual atmospheric record of the bomb curve for the Northern Hemisphere (zone 2) boreal summer<sup>22</sup>. We also grew annual plants (chia, *Salvia hispanica*) in pots at the site in spring 2021 to assess local atmosphere agreement with the atmospheric record. These were similarly analysed for Δ<sup>14</sup>C and agreed well with the atmospheric record (Δ<sup>14</sup>C = 4 ± 1‰, n = 4), being slightly higher than expected. This probably reflects extensive decomposition of recent (post-bomb) organic matter at the forest floor post-fire and some of the resulting CO<sub>2</sub> being incorporated via photosynthesis into chia tissues (Supplementary Fig. 5).

### Forward simulation of heterogeneous tree reserve carbon pools

We simulated the distribution of ages possible in sprouts with different mean ages (5, 10, 15 or 21 years) using the 'SoilR' package (version 1.0)<sup>48</sup> in R using a two-pool model (Fig. 4a). We extended the built-in atmospheric record<sup>49</sup> (to 2019) with a recent annual record<sup>22</sup> and the additional assumption that 2020 atmosphere was −4‰, consistent with the recent annual slope. The package has built-in multiple-pool models of carbon and can track carbon of different ages through these pools. Stem nonstructural carbon has previously been simplified in a model as being composed of two pools: (1) a 'fast' turnover time pool of young (recently fixed) carbon and (2) a 'slow' turnover time pool of old carbon (Fig. 4a)<sup>23</sup>. Because these redwood trees (with age at thousands of years) may be an order of magnitude older than the oldest reserves we might consider (tens to hundreds of years), have been canopy-dominant for decades and have many rings of sapwood (50–100+), we assumed steady state in simulations of reserve accumulation over 500 years within such a two-pool model with a range of turnover times and compositions. Thus, using a two-pool model (Fig. 4a), we assumed the turnover time of the young (fast) pool was 1 year ( $t_1$ ) and then simulated a range of turnover times of the old (slow) pool from 1.1 to 200 years ( $t_2$ ); pools were built over 521 years (beginning 1,500) assuming steady state, 90% annual loss of the fast pool, 10% annual transfer of carbon from the fast to the slow pool and slow pool annual loss rate of  $1/t_2$  (inverse of turnover time). We then produced 10,791 candidate mixtures of fast (99–1%;  $t_1 = 1$  year) and slow (1–99%;  $t_2 = 1.1$ –200 years) carbon. We identified mixtures of fast and slow pool carbon that produced mean Δ<sup>14</sup>C matching sprout ages of 5 (Δ<sup>14</sup>C = 12.5 ± 2‰), 10 (Δ<sup>14</sup>C = 37 ± 2‰), 15 (Δ<sup>14</sup>C = 57 ± 2‰) or 21 years (Δ<sup>14</sup>C = 85 ± 2‰; oldest sprout). These candidate mixtures are shown in Fig. 4b, although turnover times of the slow pool greater than 100 years are excluded for clarity. Finally, we calculated the age density distribution ('SystemAge()' function in SoilR) and converted this to a cumulative sum with increasing age (Fig. 4c). This allowed estimation of the percentage of reserve C greater than a given age (that is, 57 years). We repeated these simulations with a slower fast pool turnover time ( $t_1 = 5$  years), but results were only weakly sensitive to this parameter, so we report results for  $t_1 = 1$  year.

### Reporting summary

Further information on research design is available in the Nature Portfolio Reporting Summary linked to this article.

### Data availability

Radiocarbon data are provided in Supplementary Information, and other data are archived at <https://doi.org/10.5281/zenodo.10010942>.

### Code availability

Simulation code is archived at <https://doi.org/10.5281/zenodo.10010942>.

### References

- Ogle, K. & Pacala, S. W. A modeling framework for inferring tree growth and allocation from physiological, morphological and allometric traits. *Tree Physiol.* **29**, 587–605 (2009).
- Fisher, R. A. et al. Taking off the training wheels: the properties of a dynamic vegetation model without climate envelopes. *CLM4. 5* (ED). *Geosci. Model Dev.* **8**, 3593–3619 (2015).
- Koven, C. D. et al. Benchmarking and parameter sensitivity of physiological and vegetation dynamics using the Functionally Assembled Terrestrial Ecosystem Simulator (FATES) at Barro Colorado Island, Panama. *Biogeosciences* **17**, 3017–3044 (2020).
- Epron, D. et al. Pulse-labelling trees to study carbon allocation dynamics: a review of methods, current knowledge and future prospects. *Tree Physiol.* **32**, 776–798 (2012).
- Carbone, M. S. et al. Age, allocation and availability of nonstructural carbon in mature red maple trees. *New Phytol.* **200**, 1145–1155 (2013).
- Huang, J. et al. Storage of carbon reserves in spruce trees is prioritized over growth in the face of carbon limitation. *Proc. Natl Acad. Sci. USA* **118**, e2023297118 (2021).
- Speer, J. H., Swetnam, T. W., Wickman, B. E. & Youngblood, A. Changes in pandora moth outbreak dynamics during the past 622 years. *Ecology* **82**, 679–697 (2001).
- Bär, A., Michaletz, S. T. & Mayr, S. Fire effects on tree physiology. *New Phytol.* **223**, 1728–1741 (2019).
- Tanner, E. V., Rodriguez-Sanchez, F., Healey, J. R., Holdaway, R. J. & Bellingham, P. J. Long-term hurricane damage effects on tropical forest tree growth and mortality. *Ecology* **95**, 2974–2983 (2014).
- Dietze, M. C. et al. Nonstructural carbon in woody plants. *Annu. Rev. Plant Biol.* **65**, 667–687 (2014).
- Vargas, R., Trumbore, S. E. & Allen, M. F. Evidence of old carbon used to grow new fine roots in a tropical forest. *New Phytol.* **182**, 710–718 (2009).
- Koch, G. W., Sillett, S. C., Jennings, G. M. & Davis, S. D. The limits to tree height. *Nature* **428**, 851–854 (2004).
- Sillett, S. C. et al. How do tree structure and old age affect growth potential of California redwoods? *Ecol. Monogr.* **85**, 181–212 (2015).
- Curtis, P. S. et al. Biometric and eddy-covariance based estimates of annual carbon storage in five eastern North American deciduous forests. *Agric. For. Meteorol.* **113**, 3–19 (2002).
- Woodward, B. D., Romme, W. H. & Evangelista, P. H. Early postfire response of a northern range margin coast redwood forest community. *For. Ecol. Manag.* **462**, 117966 (2020).
- Brown, P. M. & Baxter, W. T. Fire history in coast redwood forests of the Mendocino Coast, California. *Northwest Sci.* **77**, 147–158 (2003).
- Brown, P. M. & Swetnam, T. W. A cross-dated fire history from coast redwood near Redwood National Park, California. *Can. J. Res.* **24**, 21–31 (1994).
- Lazzeri-Aerts, R. & Russell, W. Survival and recovery following wildfire in the southern range of the coast redwood forest. *Fire Ecol.* **10**, 43–55 (2014).

19. Safford, H. D., Paulson, A. K., Steel, Z. L., Young, D. J. N. & Wayman, R. B. The 2020 California fire season: a year like no other, a return to the past or a harbinger of the future? *Glob. Ecol. Biogeogr.* **31**, 2005–2025 (2022).
20. Stephens, S. L. & Fry, D. L. Fire history in coast redwood stands in the northeastern Santa Cruz mountains, California. *Fire Ecol.* **1**, 2–19 (2005).
21. Trumbore, S. E., Sierra, C. A. & Pries, C. H. Radiocarbon nomenclature, theory, models, and interpretation: measuring age, determining cycling rates, and tracing source pools. In *Radiocarbon and Climate Change: Mechanisms, Applications and Laboratory Techniques* (eds. Schuur, A. G. E. et al.) pp. 45–82 (Springer, 2016).
22. Hua, Q. et al. Atmospheric radiocarbon for the period 1950–2019. *Radiocarbon* **64**, 723–745 (2022).
23. Richardson, A. D. et al. Distribution and mixing of old and new nonstructural carbon in two temperate trees. *New Phytol.* **206**, 590–597 (2015).
24. Muhr, J. et al. How fresh is maple syrup? Sugar maple trees mobilize carbon stored several years previously during early springtime sap-ascent. *New Phytol.* **209**, 1410–1416 (2016).
25. D'Andrea, E. et al. Winter's bite: beech trees survive complete defoliation due to spring late-frost damage by mobilizing old C reserves. *New Phytol.* **224**, 625–631 (2019).
26. Muhr, J., Trumbore, S., Higuchi, N. & Kunert, N. Living on borrowed time—Amazonian trees use decade-old storage carbon to survive for months after complete stem girdling. *New Phytol.* **220**, 111–120 (2018).
27. Trumbore, S., Czimczik, C. I., Sierra, C. A., Muhr, J. & Xu, X. Non-structural carbon dynamics and allocation relate to growth rate and leaf habit in California oaks. *Tree Physiol.* **35**, 1206–1222 (2015).
28. Herrera-Ramírez, D. et al. Probability distributions of nonstructural carbon ages and transit times provide insights into carbon allocation dynamics of mature trees. *New Phytol.* **226**, 1299–1311 (2020).
29. Peltier, D. et al. An incubation method to determine the age of available nonstructural carbon in woody plant tissues. *Tree Physiol.* (in the press).
30. Fink, S. Some cases of delayed or induced development of axillary buds from persisting detached meristems in conifers. *Am. J. Bot.* **71**, 44–51 (1984).
31. Waters, D. A., Burrows, G. E. & Harper, J. D. *Eucalyptus regnans* (Myrtaceae): a fire-sensitive eucalypt with a resprouter epicormic structure. *Am. J. Bot.* **97**, 545–556 (2010).
32. Pausas, J. G. & Keeley, J. E. Epicormic resprouting in fire-prone ecosystems. *Trends Plant Sci.* **22**, 1008–1015 (2017).
33. Richards, J. H. et al. Tropical tree species differ in damage and mortality from lightning. *Nat. Plants* **8**, 1007–1013 (2022).
34. Schutz, A. E. N., Bond, W. J. & Cramer, M. D. Juggling carbon: allocation patterns of a dominant tree in a fire-prone savanna. *Oecologia* **160**, 235–246 (2009).
35. Bentrup, C. *Carbon Limitation of Height Growth: Evidence from Sequoia sempervirens* (Northern Arizona Univ., 2009).
36. Sillett, S. C. et al. Rangewide climatic sensitivities and non-timber values of tall *Sequoia sempervirens* forests. *For. Ecol. Manag.* **526**, 120573 (2022).
37. Sillett, S. C., Van Pelt, R., Carroll, A. L., Campbell-Spickler, J. & Antoine, M. E. Aboveground biomass dynamics and growth efficiency of *Sequoia sempervirens* forests. *For. Ecol. Manag.* **458**, 117740 (2020).
38. Douhovnikoff, V., Cheng, A. M. & Dodd, R. S. Incidence, size and spatial structure of clones in second-growth stands of coast redwood, *Sequoia sempervirens* (Cupressaceae). *Am. J. Bot.* **91**, 1140–1146 (2004).
39. PRISM Climate Group. Oregon State University. <https://prism.oregonstate.edu>. Accessed 23 Sep 2022.
40. Burgess, S. S. O. & Dawson, T. E. The contribution of fog to the water relations of *Sequoia sempervirens* (D. Don): foliar uptake and prevention of dehydration. *Plant Cell Environ.* **27**, 1023–1034 (2004).
41. Carbone, M. S. et al. Flux Puppy—an open-source software application and portable system design for low-cost manual measurements of CO<sub>2</sub> and H<sub>2</sub>O fluxes. *Agric. For. Meteorol.* **274**, 1–6 (2019).
42. Landhäusser, S. M. et al. Standardized protocols and procedures can precisely and accurately quantify non-structural carbohydrates. *Tree Physiol.* **38**, 1764–1778 (2018).
43. Lowe, D. C. Preparation of graphite targets for radiocarbon dating by tandem accelerator mass spectrometer (TAMS). *Int. J. Appl. Radiat. Isot.* **35**, 349–352 (1984).
44. Vogel, J. S., Southon, J. R., Nelson, D. E. & Brown, T. A. Performance of catalytically condensed carbon for use in accelerator mass spectrometry. *Nucl. Instrum. Methods Phys. Res. B* **5**, 289–293 (1984).
45. Synal, H.-A., Stocker, M. & Suter, M. MICADAS: a new compact radiocarbon AMS system. *Nucl. Instrum. Methods Phys. Res. B* **259**, 7–13 (2007).
46. Stuiver, M. & Polach, H. A. Discussion reporting of <sup>14</sup>C data. *Radiocarbon* **19**, 355–363 (1977).
47. Reimer, P. J., Brown, T. A. & Reimer, R. W. Discussion: reporting and calibration of post-bomb <sup>14</sup>C data. *Radiocarbon* **46**, 1299–1304 (2004).
48. Sierra, C. A., Müller, M. & Trumbore, S. E. Modeling radiocarbon dynamics in soils: SoilR version 1.1. *Geosci. Model Dev.* **7**, 1919–1931 (2014).
49. Reimer, P. J. et al. IntCal13 and Marine13 radiocarbon age calibration curves 0–50,000 years cal BP. *Radiocarbon* **55**, 1869–1887 (2013).

## Acknowledgements

This work was funded by NSF-IOS-RAPID number 2053337 and grant number 149 from the Save-the-Redwoods League. The incubation method we used was developed under NSF-IOS-RAPID number 1936205. We thank J. Kerbavaz and the staff at BBRSP for allowing research access soon after the fire. We thank J. Campbell-Spickler for assistance in installing canopy PhenoCams. We gratefully acknowledge the financial support of the Office of the President and Vice President of Research at Northern Arizona University for acquisition of the MICADAS.

## Author contributions

M.S.C., G.K. and A.D.R. conceived of the study. M.E. surveyed and selected study trees, and G.K., A.D.R., J.L., M.E. and D.M.P.P. collected the data. M.C.M. and A.M.T. contributed additional carbohydrate measurements and analysis. D.M.P.P., M.S.C. and A.D.R. analysed the data, and D.M.P.P. wrote the first draft of the manuscript with M.S.C., G.K. and A.D.R. All authors substantially contributed to revisions.

## Competing interests

The authors declare no competing interests.

## Additional information

**Supplementary information** The online version contains supplementary material available at <https://doi.org/10.1038/s41477-023-01581-z>.

**Correspondence and requests for materials** should be addressed to Drew M. P. Peltier.

**Peer review information** *Nature Plants* thanks Jordi Martinez-Vilalta, Frida Piper and Adrian Rocha for their contribution to the peer review of this work.

**Reprints and permissions information** is available at [www.nature.com/reprints](http://www.nature.com/reprints).

**Publisher's note** Springer Nature remains neutral with regard to jurisdictional claims in published maps and institutional affiliations.

Springer Nature or its licensor (e.g. a society or other partner) holds exclusive rights to this article under a publishing agreement with the author(s) or other rightsholder(s); author

self-archiving of the accepted manuscript version of this article is solely governed by the terms of such publishing agreement and applicable law.

© The Author(s), under exclusive licence to Springer Nature Limited 2023



## Reporting Summary

Nature Portfolio wishes to improve the reproducibility of the work that we publish. This form provides structure for consistency and transparency in reporting. For further information on Nature Portfolio policies, see our [Editorial Policies](#) and the [Editorial Policy Checklist](#).

### Statistics

For all statistical analyses, confirm that the following items are present in the figure legend, table legend, main text, or Methods section.

n/a Confirmed

- |                                     |                                     |  |
|-------------------------------------|-------------------------------------|--|
| <input type="checkbox"/>            | <input checked="" type="checkbox"/> | The exact sample size ( $n$ ) for each experimental group/condition, given as a discrete number and unit of measurement  |
| <input type="checkbox"/>            | <input checked="" type="checkbox"/> | A statement on whether measurements were taken from distinct samples or whether the same sample was measured repeatedly  |
| <input type="checkbox"/>            | <input checked="" type="checkbox"/> | The statistical test(s) used AND whether they are one- or two-sided<br><i>Only common tests should be described solely by name; describe more complex techniques in the Methods section.</i>   |
| <input type="checkbox"/>            | <input checked="" type="checkbox"/> | A description of all covariates tested   |
| <input type="checkbox"/>            | <input checked="" type="checkbox"/> | A description of any assumptions or corrections, such as tests of normality and adjustment for multiple comparisons  |
| <input type="checkbox"/>            | <input checked="" type="checkbox"/> | A full description of the statistical parameters including central tendency (e.g. means) or other basic estimates (e.g. regression coefficient) AND variation (e.g. standard deviation) or associated estimates of uncertainty (e.g. confidence intervals) |
| <input type="checkbox"/>            | <input checked="" type="checkbox"/> | For null hypothesis testing, the test statistic (e.g. $F$ , $t$ , $r$ ) with confidence intervals, effect sizes, degrees of freedom and $P$ value noted<br><i>Give <math>P</math> values as exact values whenever suitable.</i>                            |
| <input checked="" type="checkbox"/> | <input type="checkbox"/>            | For Bayesian analysis, information on the choice of priors and Markov chain Monte Carlo settings   |
| <input checked="" type="checkbox"/> | <input type="checkbox"/>            | For hierarchical and complex designs, identification of the appropriate level for tests and full reporting of outcomes   |
| <input checked="" type="checkbox"/> | <input type="checkbox"/>            | Estimates of effect sizes (e.g. Cohen's $d$ , Pearson's $r$ ), indicating how they were calculated   |

*Our web collection on [statistics for biologists](#) contains articles on many of the points above.*

### Software and code

Policy information about [availability of computer code](#)

Data collection

Data analysis

For manuscripts utilizing custom algorithms or software that are central to the research but not yet described in published literature, software must be made available to editors and reviewers. We strongly encourage code deposition in a community repository (e.g. GitHub). See the Nature Portfolio [guidelines for submitting code & software](#) for further information.

### Data

Policy information about [availability of data](#)

All manuscripts must include a [data availability statement](#). This statement should provide the following information, where applicable:

- Accession codes, unique identifiers, or web links for publicly available datasets
- A description of any restrictions on data availability
- For clinical datasets or third party data, please ensure that the statement adheres to our [policy](#)

## Research involving human participants, their data, or biological material

Policy information about studies with [human participants or human data](#). See also policy information about [sex, gender \(identity/presentation\), and sexual orientation](#) and [race, ethnicity and racism](#).

Reporting on sex and gender	N/A
Reporting on race, ethnicity, or other socially relevant groupings	N/A
Population characteristics	N/A
Recruitment	N/A
Ethics oversight	N/A

Note that full information on the approval of the study protocol must also be provided in the manuscript.

## Field-specific reporting

Please select the one below that is the best fit for your research. If you are not sure, read the appropriate sections before making your selection.

Life sciences     Behavioural & social sciences     Ecological, evolutionary & environmental sciences

For a reference copy of the document with all sections, see [nature.com/documents/nr-reporting-summary-flat.pdf](https://www.nature.com/documents/nr-reporting-summary-flat.pdf)

## Ecological, evolutionary & environmental sciences study design

All studies must disclose on these points even when the disclosure is negative.

Study description	In early 2021 we covered small basal buds on burnt trees to exclude light (arresting photosynthesis) and ensure sprouts were grown entirely using stored carbon reserves. Sprouting began 4 months after fire, and we collected sprouts over the following six months. We used radiocarbon (Del14C) to determine the mean age (or, time since photosynthetic fixation) of sprout carbon by reference to the atmospheric bomb spike.
Research sample	60 old-growth coast redwood ( <i>Sequoia sempervirens</i> ) trees that were damaged by fire were selected for this study. A subset of 18 of these trees spanning the range of tree sizes in the larger group of trees was selected for direct observation of carbon reserve age using increment cores.
Sampling strategy	We covered small basal buds on burnt trees to exclude light on 60 trees spread across the park. Given extremely limited access post-fire due to potentially hazardous conditions, this was a very large sample size representing significant effort.
Data collection	We collected sprouts every few months and measured the Del14C of the carbon in these sprouts using Accelerator Mass Spectrometry. ME surveyed and selected study trees and GK, AR, JL, ME, and DP collected the data. MCM and AMT contributed additional NSC measurements and analysis. DP, MC, and AR analyzed the data.
Timing and spatial scale	We collected sprouts in February, March, April, and July of 2021. Essentially as soon as we could access the site and roughly monthly into the summer growing season.  We collected increment cores in April 2021 and April 2022. These corresponded to spring when reserves might be highest.
Data exclusions	We excluded very negative Del14C values indicating contamination of sprout samples with burnt ash from the fire. We excluded observations from a single tree with fire-damaged sapwood from certain supplementary analyses, but report fits and R2 for both including/excluding this data point so that readers may independently assess.
Reproducibility	For the oldest sprouts we measured up to 4 replicates from different sprouts on the same tree to ensure values were reproducible. These values were averaged in Fig. 2. We also repeated increment core measurements in two years to ensure they were consistent.
Randomization	This is not relevant to our study as we were simply trying to characterize the age of carbon reserves used in a range of trees to recover from fire.
Blinding	Blinding is not relevant to this study.
Did the study involve field work?	<input checked="" type="checkbox"/> Yes <input type="checkbox"/> No

## Field work, collection and transport

Field conditions	Big Basin Redwoods State Park (37.1723, -122.2219) is the oldest state park in California, USA, established in 1902 protect old-growth redwood groves, which cover 4400 hectares. The park features the continuous stands of ancient (1,000-2,500 y old) redwoods south of San Francisco and the tallest tree at BBRSP ("Mother of the Forest") previously exceeded 100 m prior to storm damage (now ~ 90 m); three of the trees we sampled exceed 80 m in height. Mean annual precipitation at the park is 490 mm, mean daily temperature is 20.2 C in July and -0.3 C in January (1991-2020 normals 39). Significant additional moisture inputs occur through frequent fog events 40.
Location	Big Basin Redwoods State Park (37.1723, -122.2219)
Access & import/export	State of California Natural Resources Agency Department of Parks and Recreation gave the permit for this work. We minimized site visits and were in constant contact with Park staff. Our impacts were extremely minimal, and sections depicted in Fig. 4 were collected off trail on fallen trees hidden from view with approval from Joanne Kerbavaz · Senior Environmental Scientist at California State Parks
Disturbance	The only disturbance was the collection of a few partial sections. However, this was in an area being cleared of fallen debris using chainsaws by the park. So disturbance was entirely negligible.

## Reporting for specific materials, systems and methods

We require information from authors about some types of materials, experimental systems and methods used in many studies. Here, indicate whether each material, system or method listed is relevant to your study. If you are not sure if a list item applies to your research, read the appropriate section before selecting a response.

### Materials & experimental systems

n/a	Included in the study
<input checked="" type="checkbox"/>	<input type="checkbox"/> Antibodies
<input checked="" type="checkbox"/>	<input type="checkbox"/> Eukaryotic cell lines
<input checked="" type="checkbox"/>	<input type="checkbox"/> Palaeontology and archaeology
<input checked="" type="checkbox"/>	<input type="checkbox"/> Animals and other organisms
<input checked="" type="checkbox"/>	<input type="checkbox"/> Clinical data
<input checked="" type="checkbox"/>	<input type="checkbox"/> Dual use research of concern
<input type="checkbox"/>	<input checked="" type="checkbox"/> Plants

### Methods

n/a	Included in the study
<input checked="" type="checkbox"/>	<input type="checkbox"/> ChIP-seq
<input checked="" type="checkbox"/>	<input type="checkbox"/> Flow cytometry
<input checked="" type="checkbox"/>	<input type="checkbox"/> MRI-based neuroimaging

## Dual use research of concern

Policy information about [dual use research of concern](#)

### Hazards

Could the accidental, deliberate or reckless misuse of agents or technologies generated in the work, or the application of information presented in the manuscript, pose a threat to:

No	Yes
<input checked="" type="checkbox"/>	<input type="checkbox"/> Public health
<input checked="" type="checkbox"/>	<input type="checkbox"/> National security
<input checked="" type="checkbox"/>	<input type="checkbox"/> Crops and/or livestock
<input checked="" type="checkbox"/>	<input type="checkbox"/> Ecosystems
<input checked="" type="checkbox"/>	<input type="checkbox"/> Any other significant area

## Experiments of concern

Does the work involve any of these experiments of concern:

No	Yes
<input checked="" type="checkbox"/>	<input type="checkbox"/> Demonstrate how to render a vaccine ineffective
<input checked="" type="checkbox"/>	<input type="checkbox"/> Confer resistance to therapeutically useful antibiotics or antiviral agents
<input checked="" type="checkbox"/>	<input type="checkbox"/> Enhance the virulence of a pathogen or render a nonpathogen virulent
<input checked="" type="checkbox"/>	<input type="checkbox"/> Increase transmissibility of a pathogen
<input checked="" type="checkbox"/>	<input type="checkbox"/> Alter the host range of a pathogen
<input checked="" type="checkbox"/>	<input type="checkbox"/> Enable evasion of diagnostic/detection modalities
<input checked="" type="checkbox"/>	<input type="checkbox"/> Enable the weaponization of a biological agent or toxin
<input checked="" type="checkbox"/>	<input type="checkbox"/> Any other potentially harmful combination of experiments and agents

## Plants

Seed stocks	<input type="text" value="N/A"/>
Novel plant genotypes	<input type="text" value="N/A"/>
Authentication	<input type="text" value="N/A"/>